Friday, July 31, 2015

"Heusler Alloys for Spintronic Devices"
organized by The Center for Spintronic Materials, Interfaces, and Novel Architectures (C-SPIN)

Interface-induced perpendicular magnetic anisotropy and giant tunnel magnetoresistance in Co_2FeAl Heusler alloy based heterostructures

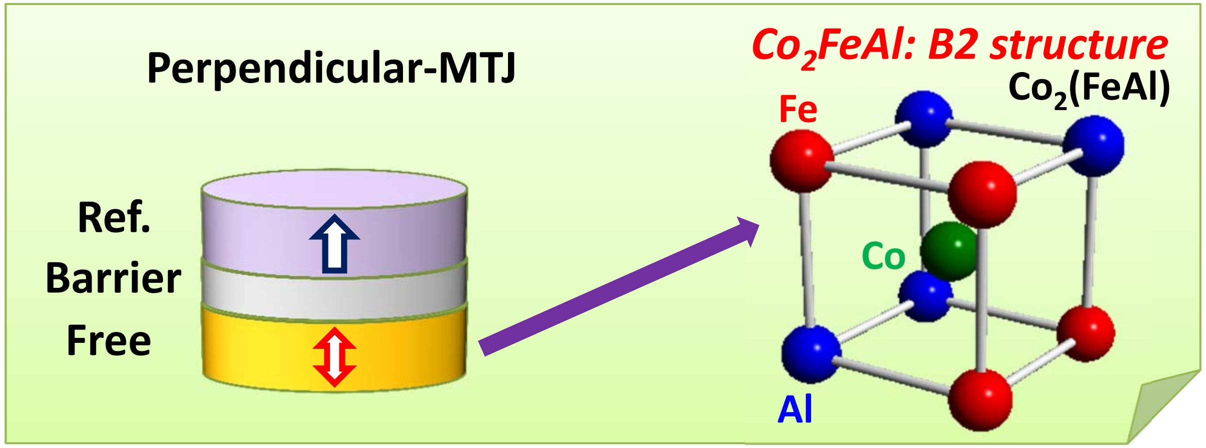

Hiroaki Sukegawa

National Institute for Materials Science (NIMS), Tsukuba, Japan

In collaboration with Magnetic Materials Unit members in NIMS:
S. Mitani, K. Inomata , Z. C. Wen (~2015.4 now Tohoku Univ. Japan), T. Scheike, T. Furubayashi, J. P. Hadorn, T. Ohkuboand K. Hono

University of Minnesota, Minneapolis, Minnesota, USA, July 30-31, 2015

NIMS: National Institute for Materials Science, Tsukuba, Japan (permanent staffs: 410, total ~1,500)

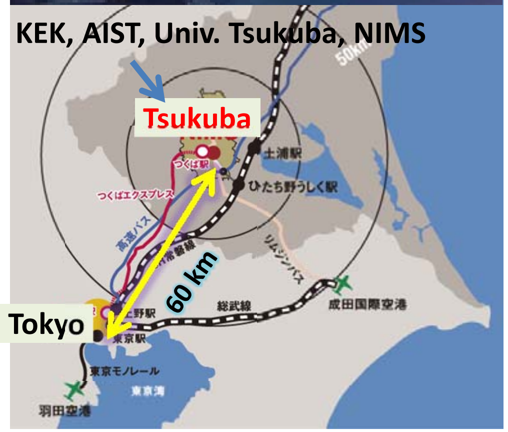

Magnetic Materials Unit

Director

Kazuhiro Hono

Magnetic Materials Group
Spintronics Group
Nanostructure Analysis Group

Spintronics group members

GL Leader

S. Mitani

NIMS Staff

S. Kasai

M. Hayashi

H. Sukegawa

Emeritus Fellow

K. Inomata

Post-Doc

P. Sheng

M. Belmoubarik

Graduate Student (Univ. of Tsukuba)

S. Hirayama

T. Scheike

Q. Xiang

Visiting Researcher

S. Ichikawa

Visiting Researcher

R. Pérez

Y. Kato

Internship

C. Choi

Technical Assist.

H. Shimadu

Admin.

A. Tomaru

Equipment

Thin-film deposition systems

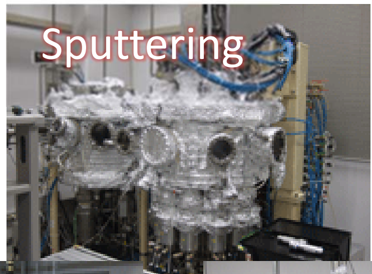

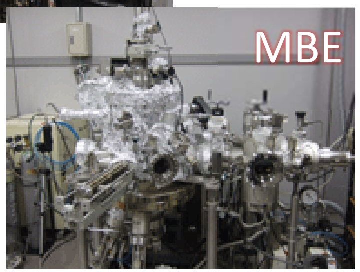

Microfab. facility

E-beam lithography

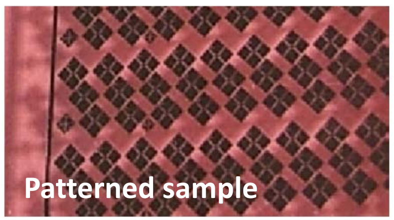

Electric measurement

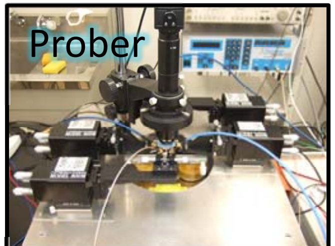

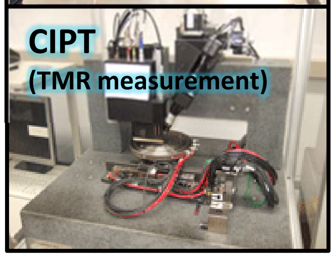

Outline

1. Background
   Co$_2$FeAl Heusler alloy based magnetic tunnel junctions (MTJs) for MRAM applications

2. Perpendicular anisotropy in Co$_2$FeAl ultra-thin films
   2.1 Perpendicular magnetic anisotropy (PMA) and TMR in ultrathin Co$_2$FeAl/MgO structures
   2.2 Enhanced PMA by Ru(02$\bar{2}$3) underlayer
   2.3 Possible mechanism of PMA

3. Co$_2$FeAl MTJs with a lattice-matched MgAl$_2$O$_4$ coherent barrier

MRAM (magnetoresistive random access memory)

C. Chappert, A. Fert and F. N. V. Dau, Nat. Mater. **6**, 813 (2007)

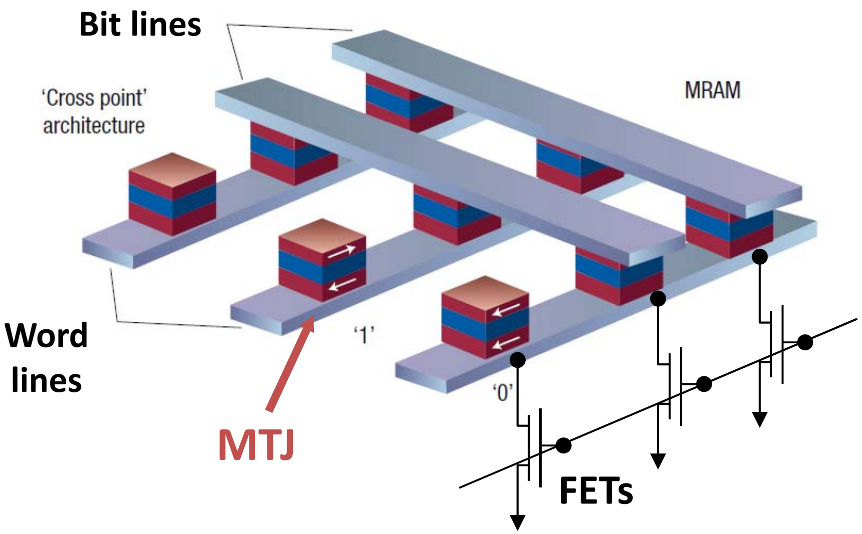

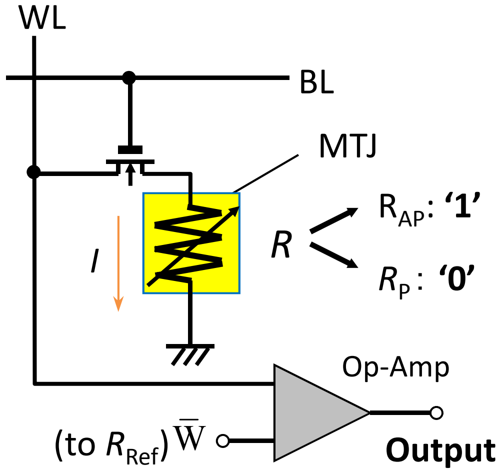

- **Nonvolatile**
- **Infinite endurance**
- High speed
- High density

MTJ (magnetic tunnel junction)

(in-plane mag. type)

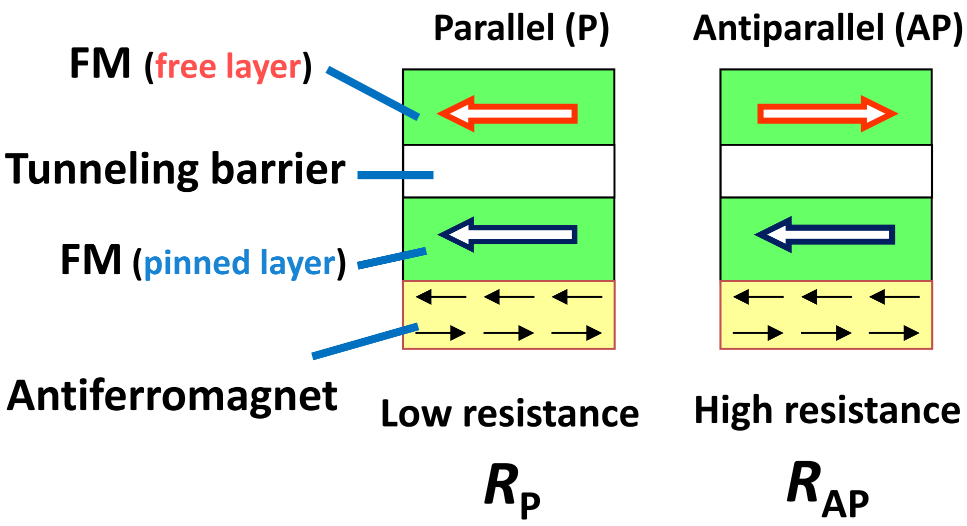

FM: Ferromagnet

TMR (tunnel magnetororesistance)

$$\text{TMR ratio} = \frac{R_{AP} - R_P}{R_P}$$

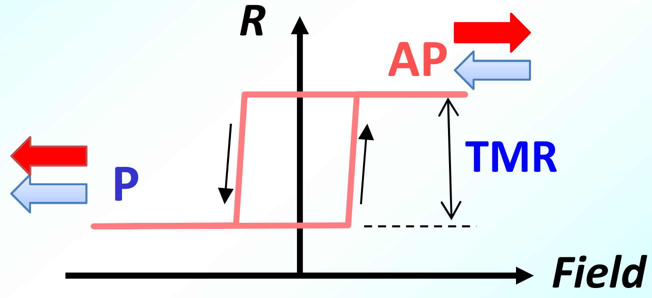

High TMR ⇨ **High output (high speed reading)**

Properties needed for MRAM application

(1) High signal output (TMR) with tunable device resistance

- ✓ High spin polarization materials
  --- Co-based Heusler alloys
- ✓ New (coherent) tunneling barrier materials
  --- $MgAl_2O_4$ based barrier

(2) High thermal stability of stored information

- ✓ High perpendicular magnetic anisotropy (PMA)
  - ➢ Bulk-induced anisotropy
    --- Multilayers, $L1_0/D0_{22}$ based alloys…
  - ➢ Interface-induced anisotropy
    --- ultrathin FM/insulator interface

(3) Low writing energy (low current density for STT writing)

- ✓ Low magnetic damping materials
  --- Co-based Heusler alloys
  --- Mn-based PMA alloys

(4) New writing technology

- ✓ Magnetic anisotropy control by electric field
- ✓ Spin-orbit torque
  - ➢ Interface PMA system

Half-metallic full Heusler alloys

$L2_1$
X_2YZ

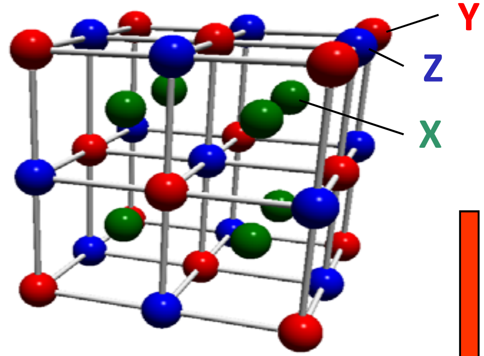

Disordered structures

***B2*: X (Y, Z)**

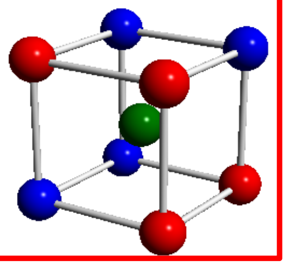

***A2*: (X, Y, Z)**
bcc structure

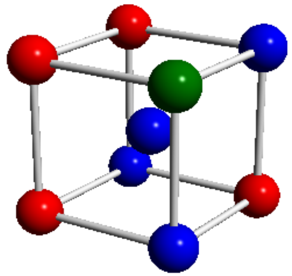

Site disordering

Lower *P*

Co-based Heusler alloy: Co_2YZ

- High Curie temperatures
- High spin polarization
- Low magnetic damping
  even in *B2* structure

Slater-Pauling rule $M_t = Z_v - 24$

● **Half-metallic material**

After I. Galanakis, PRB **66**, 174429 (2002)

Co_2FeSi S. Wumehl *et al (PRB, 2005)*

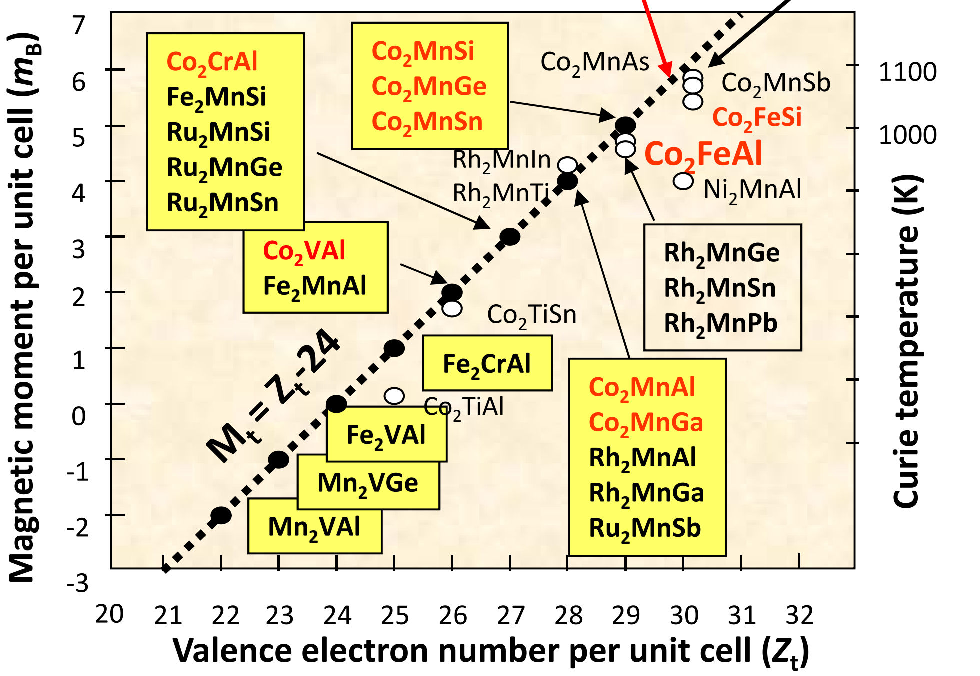

Band structure of half-metals

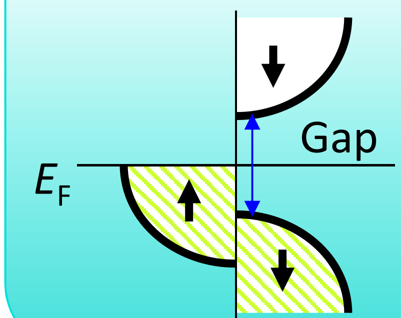

$P = 1$

TMR: infinite

Co_2FeAl (CFA) Heusler alloy for spintronics

***L*2$_1$ (X_2YZ)**

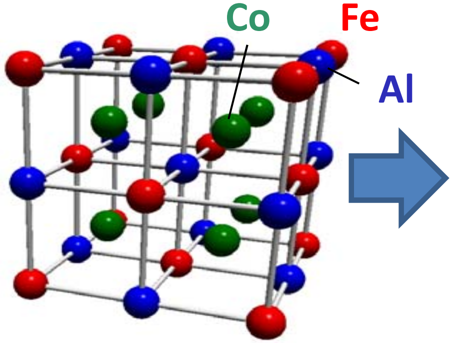

***B*2 (disordering Fe-Al)**

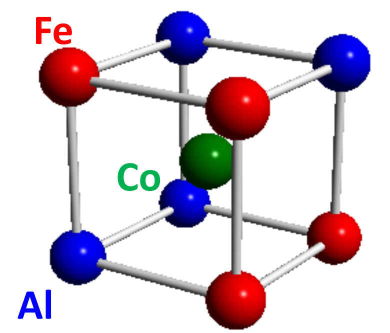

***B*2-ordered CFA is generally obtained by sputtering deposition.**

Band calculation

W. H. Wang *et al.*, PRB**81**, 140402(R) (2010).

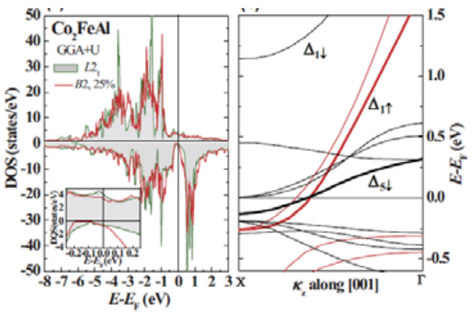

Not a perfect half-metal, but fully spin-polarized Δ_1 band

AMR

Y. Sakuraba *et al.*, APL**104**, 172407 (2014).

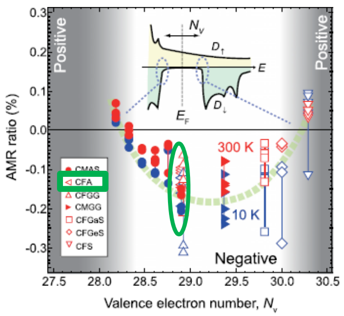

Negative AMR in B2-CFA film: a nearly half-metallic band structure

1. Small lattice misfit of CFA/MgO(001)

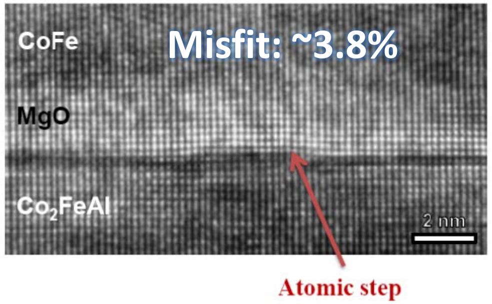

High-quality CFA/MgO-MTJs can be fabricated using a **sputtering method**.

2. Large TMR in CFA/MgO MTJs

Epitaxial CFA/MgO/CoFe(0.5 nm)/CFA (in-plane mag.)

TMR: 785% (10 K), 360% (RT)

W. H. Wang, HS *et al.*, PRB**82**, 092402 (2010).

- High spin polarization and coherent tunneling
- Less temperature dependence of TMR ratio

3. Possible low damping constant α

α ~ 0.001 for 50-nm-thick CFA(001)

S. Mizukami *et al.*, JAP**105**, 07D306 (2009). (Tohoku group)

Effective for spin-transfer torque (STT) switching

Outline

1. Background
   Co_2FeAl Heusler alloy based magnetic tunnel junctions (MTJs) for MRAM applications

2. Perpendicular anisotropy in Co_2FeAl ultra-thin films
   2.1 Perpendicular magnetic anisotropy (PMA) and TMR in ultrathin Co_2FeAl/MgO structures
   2.2 Enhanced PMA by Ru($02\bar{2}3$) underlayer
   2.3 Possible PMA mechanism

3. Co_2FeAl MTJs with a lattice-matched $MgAl_2O_4$ coherent barrier

Perpendicular MTJs

Perpendicular magnetic anisotropy (PMA)

PMA: higher thermal stability, lower STT switching current density

Bulk-induced PMA: b-PMA

Bulk PMA materials, Multilayers

$L1_0$-FePt, $D0_{22}$-MnGa, amorphous-TbFeCo, $(Co/Pt)_n$, $(Co/Pd)_n$…

Small uniaxial magnetocrystalline anisotropy can be expected in bulk of **cubic** Heusler alloys.

→Use of Interface effect

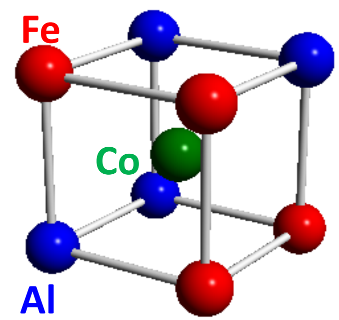

Interface-induced PMA: i-PMA

Interface at ultrathin layer and oxide

Pt/Co/AlOx trilayers

B. Rodmacq *et al.*, PRB **79**, 024423 (2009).

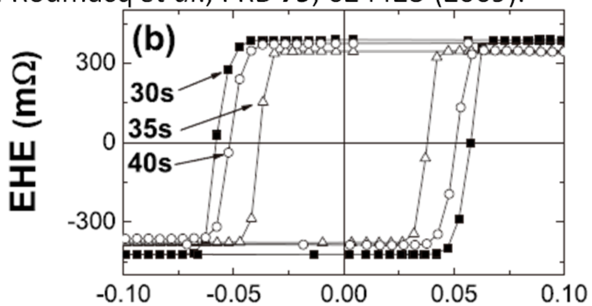

CoFeB(1)/MgO(0.9)/CoFeB(1.3 nm) p-MTJ

S. Ikeda *et al.*, Nat. Mater. **9**, 721 (2010).

TMR ratio = 120%

K_u = 2.1×10^6 erg/cm^3

$\boldsymbol{J_{c0}}$ **= 3.6 MA/cm²**

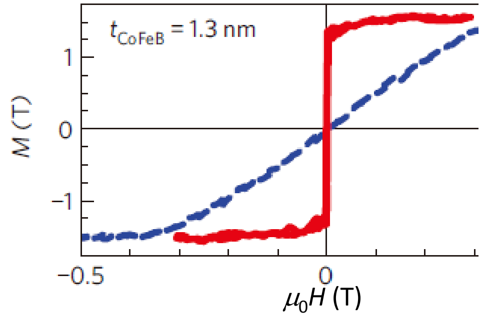

Ultra-thin Co_2FeAl (CFA)/MgO structure

Perpendicular magnetization of Co_2FeAl (CFA) ultrathin films

MgO(001) sub./Cr/CFA(t nm)/MgO/Pt

***M–H* curves**

***t* = 0.8 nm: perpendicular**

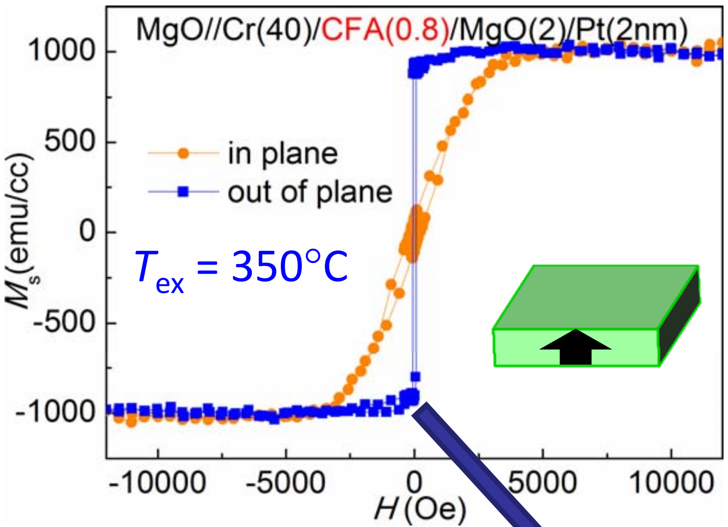

***t* = 1.6 nm: in-plane**

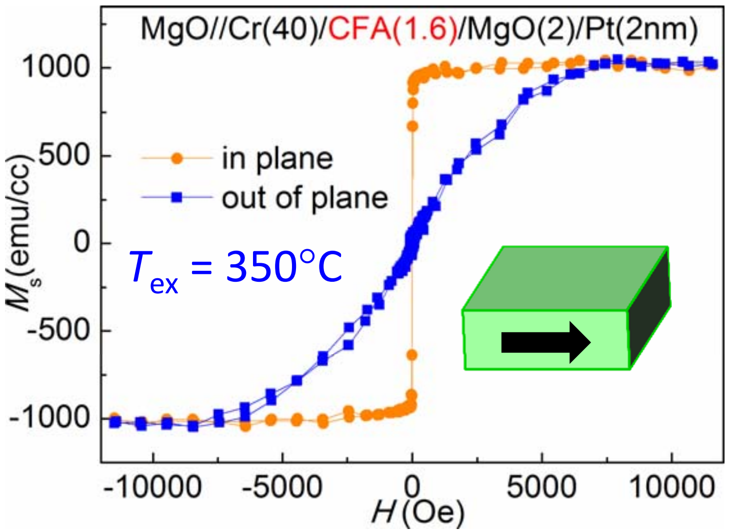

Area enclosed by the curves: PMA energy density (K_u)

Sputter deposition

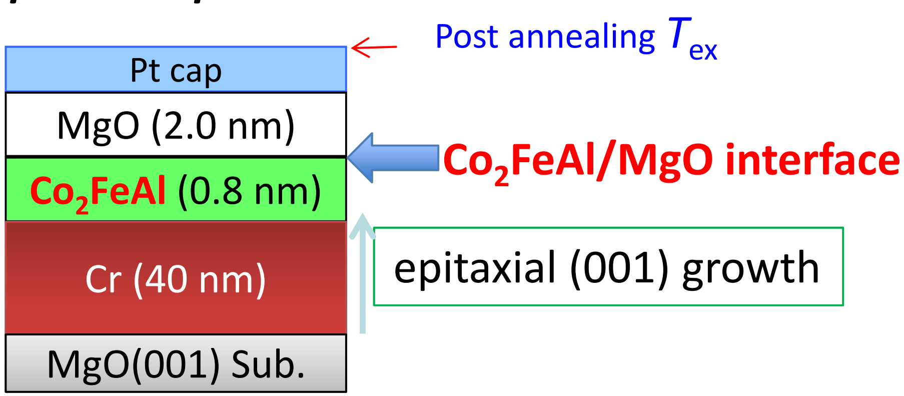

Wen *et al.*, APL**98**, 242507(2011).

K_u = 2×10⁶ erg/cm³ (×10⁵ J/m³)

Cf. CoFeB/MgO: **2~5×10⁶ erg/cm³** (×10⁵ J/m³)

*M. Yamanouchi *et al.*, J. Appl. Phys. **109**, 07C712 (2011).

i-PMA at an ultrathin Co_2FeAl (CFA)/MgO interface

T_{ex} = 300°C

MgO(001) sub./Cr/CFA(*t* nm)/MgO/Pt

Saturation magnetization M_s

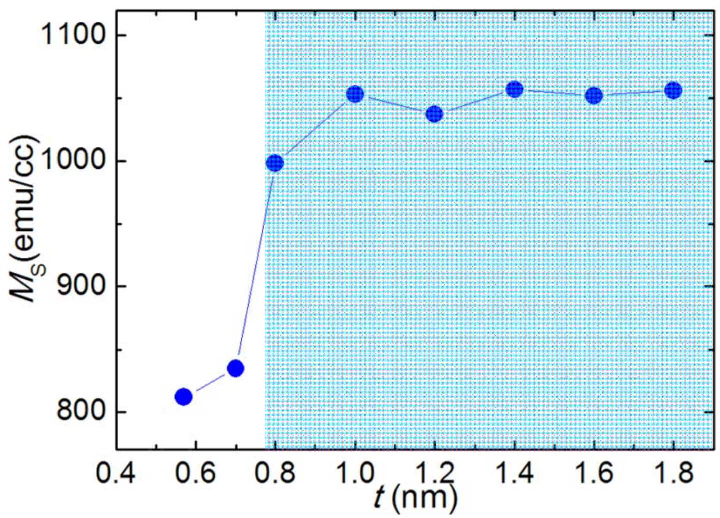

$K_u t$ vs. t

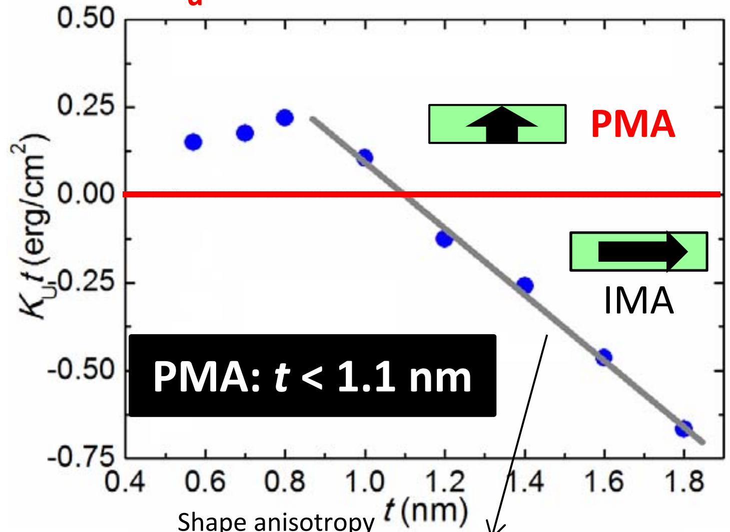

t > 0.8 nm: M_s > 1000 emu/cm³

Shape anisotropy

$$K_u t = (K_V - 2\pi M_S^2)t + K_s$$

slope intercept

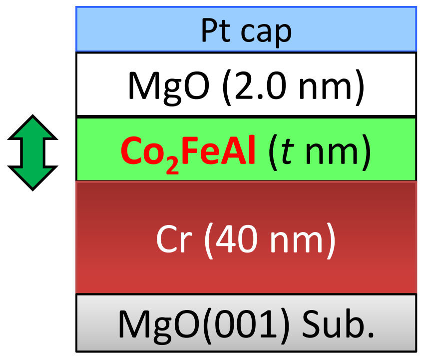

Post annealing T_{ex}

Bulk PMA energy density K_V

K_v = −2.6×10⁶ erg/cm³ (×10⁵ J/m³) In-plane (mainly lattice distortion)

Interfacial PMA energy density K_s

K_s = +1.04 erg/cm² (mJ/m²) **Perpendicular**

CFA/MgO interface induces PMA

Z. C. Wen *et al.*, APL**98**, 242507 (2011).

CFA/MgO/CoFeB p-MTJs on MgO(001)

Wen *et al.*, APEX**5**, 063003 (2012).

MTJs: Cr/CFA(1.0 nm)/MgO/Fe/$Co_{20}Fe_{60}B_{20}$

improvement of the interface structure

T_{ex}= 325°C

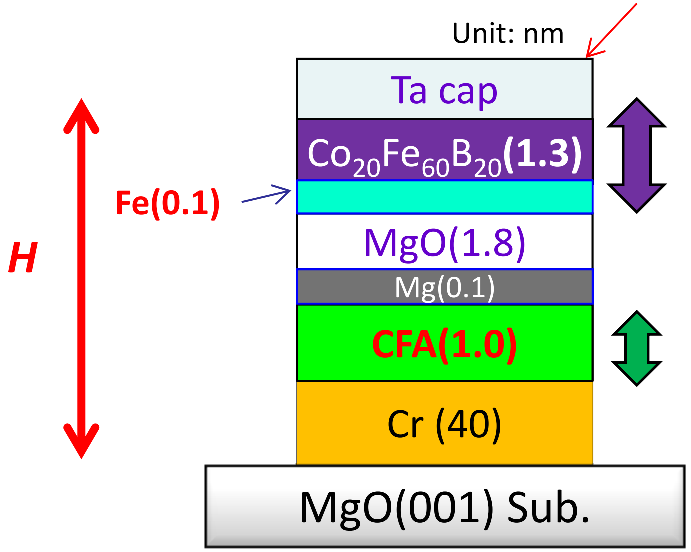

TMR curve

Area: 10x5μm²

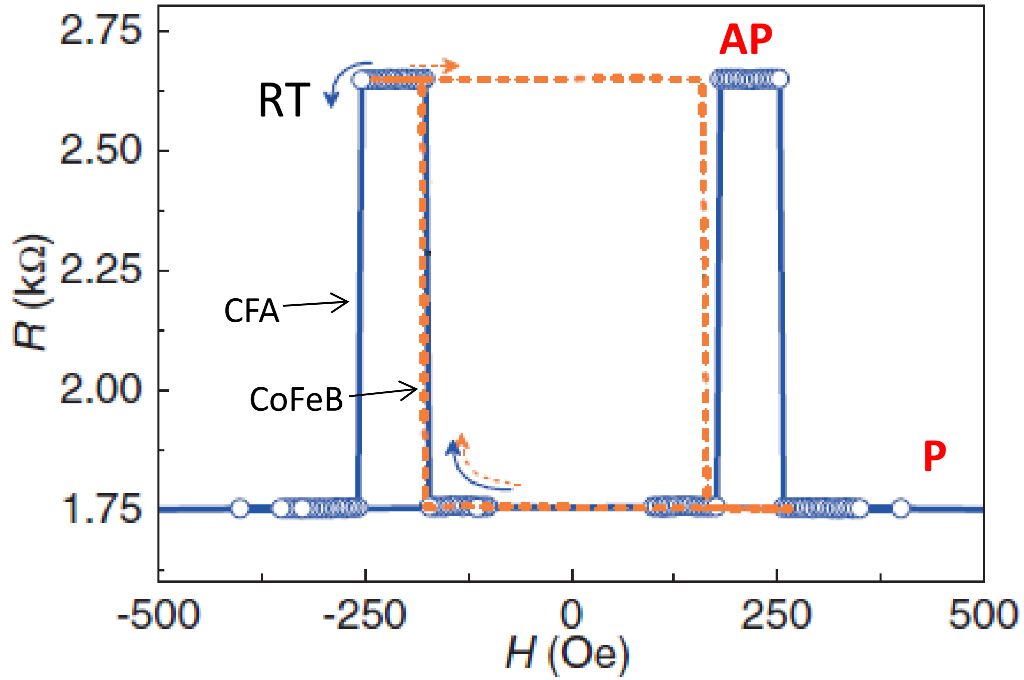

perp-TMR at RT = 53% ~ 91%

Ultra-thin CFA (~1 nm) still has a high effective spin polarization.

Outline

1. Background
   Co_2FeAl Heusler alloy based magnetic tunnel junctions (MTJs) for MRAM applications

2. Perpendicular anisotropy in Co_2FeAl ultra-thin films
   - 2.1 Perpendicular magnetic anisotropy (PMA) and TMR in ultrathin Co_2FeAl/MgO structures
   - **2.2 Enhanced PMA by Ru($02\bar{2}3$) underlayer**
   - 2.3 Possible PMA mechanism

3. Co_2FeAl MTJs with a lattice-matched $MgAl_2O_4$ coherent barrier

Enhanced PMA in a Ru-buffered CFA/MgO

t_{CFA} = 1 nm

Z. C. Wen *et al.*, Adv. Mater. **26**, 6483 (2014).

Cr(40)/CFA(1.0)/MgO(2 nm)

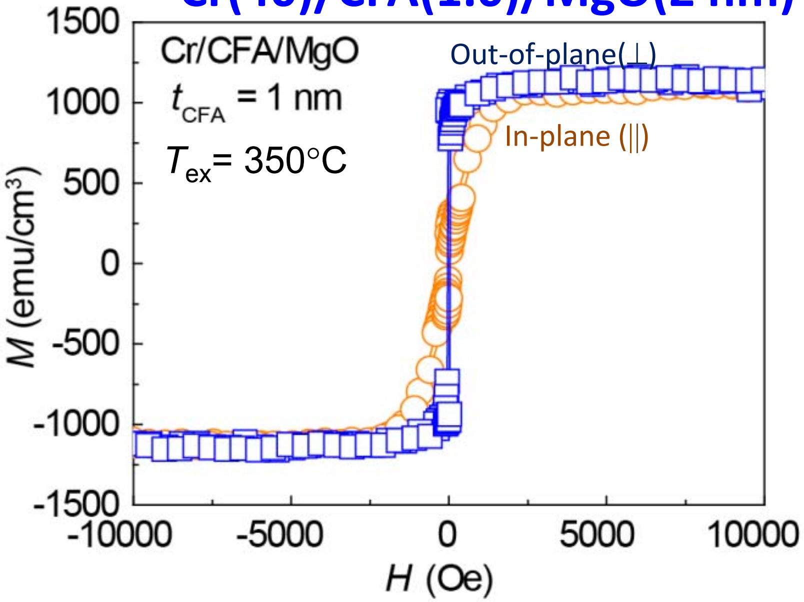

Ru(40)/CFA(1.0)/MgO(1.8 nm)

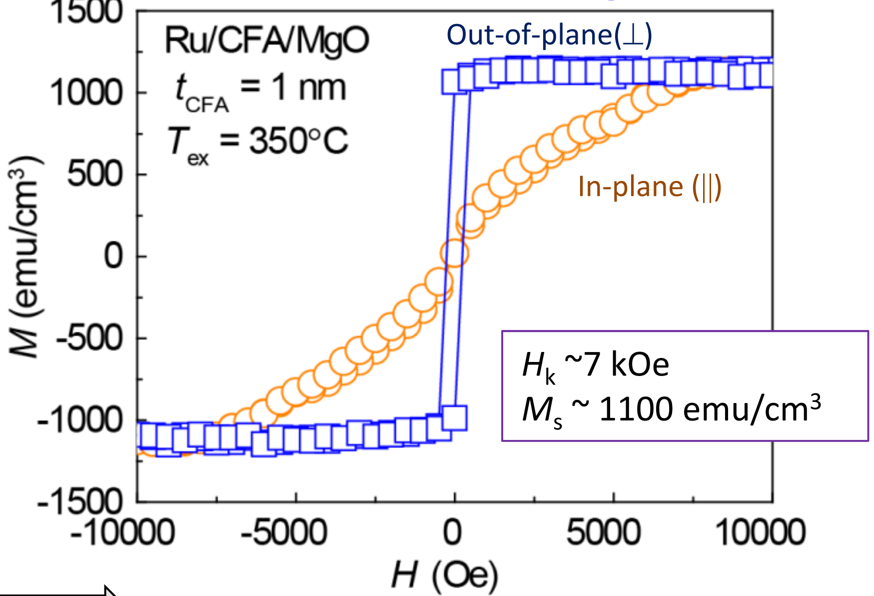

$\boldsymbol{K_u}$ Cr-buffer: 0.8×10^6 erg/cm^3 (×10^5 J/m^3) → 4 times → $\boldsymbol{K_u}$ Ru-buffer: 3.1×10^6 erg/cm^3 (×10^5 J/m^3)

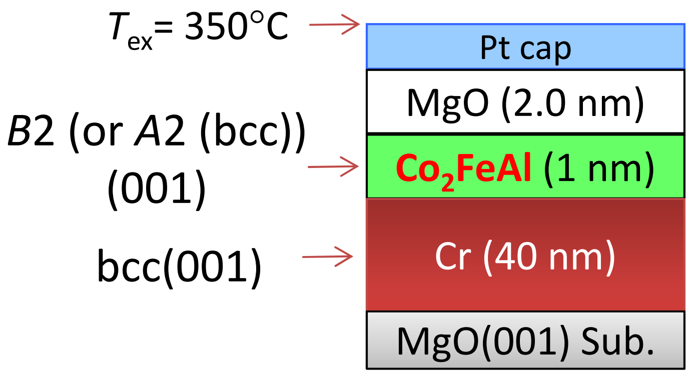

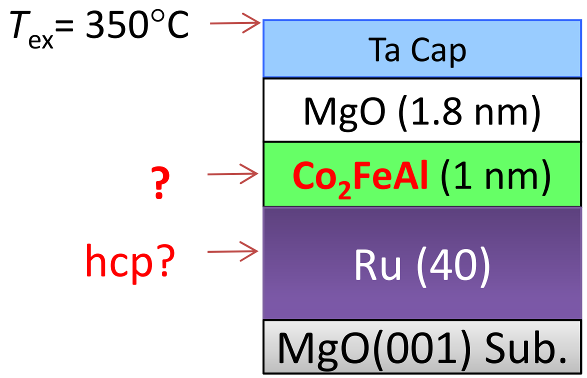

Enhancement of PMA using the Ru buffer

K_s(Cr-buffered) = 1.0 erg/cm^2
K_s(Ru-buffered) = 2.2 erg/cm^2

XRD profiles of Ru-buffered CFA on MgO

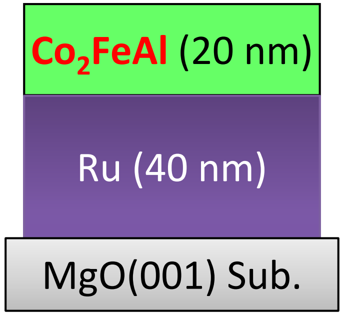

Out-of-plane (2θ-ω scan)

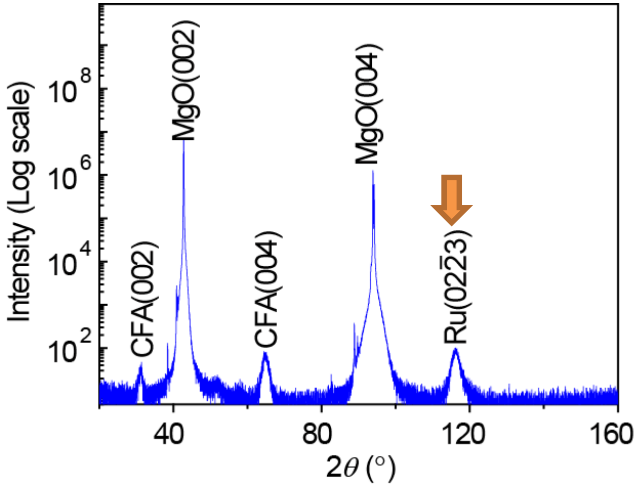

Ru: Only (02$\bar{2}$3), CFA: only (00*L*)

Pole scan for Ru

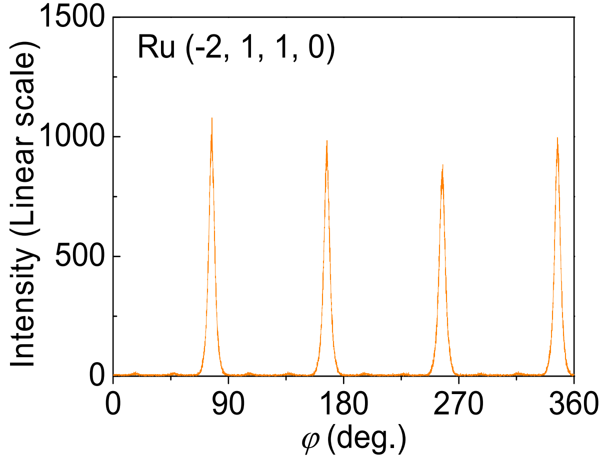

4-fold peaks for Ru: mixture of variants

Epitaxial growth of *4-fold symmetry* Ru(02$\bar{2}$3) on MgO(001)

Pole scan for CFA

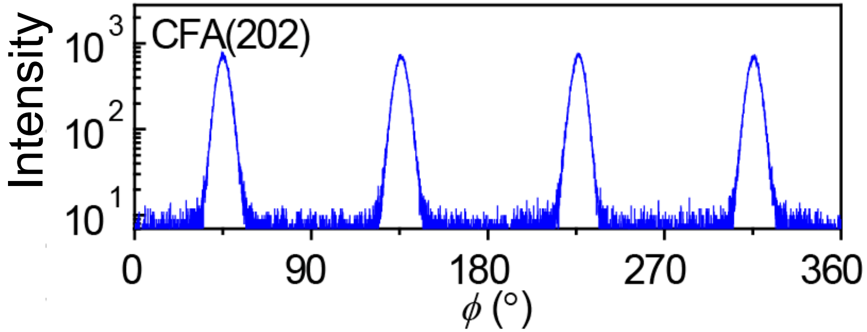

Epitaxial growth of *B*2-ordered CFA(001) on Ru(02$\bar{2}$3)

HRTEM image of Ru-buffered CFA on MgO

Ru (40)/CFA (1.2)/MgO (1.8)/[Fe (0.1)/CoFeB (1.3 nm)]

Amo?

rock-salt (001)

bcc (001)

hcp $(02\bar{2}3)$

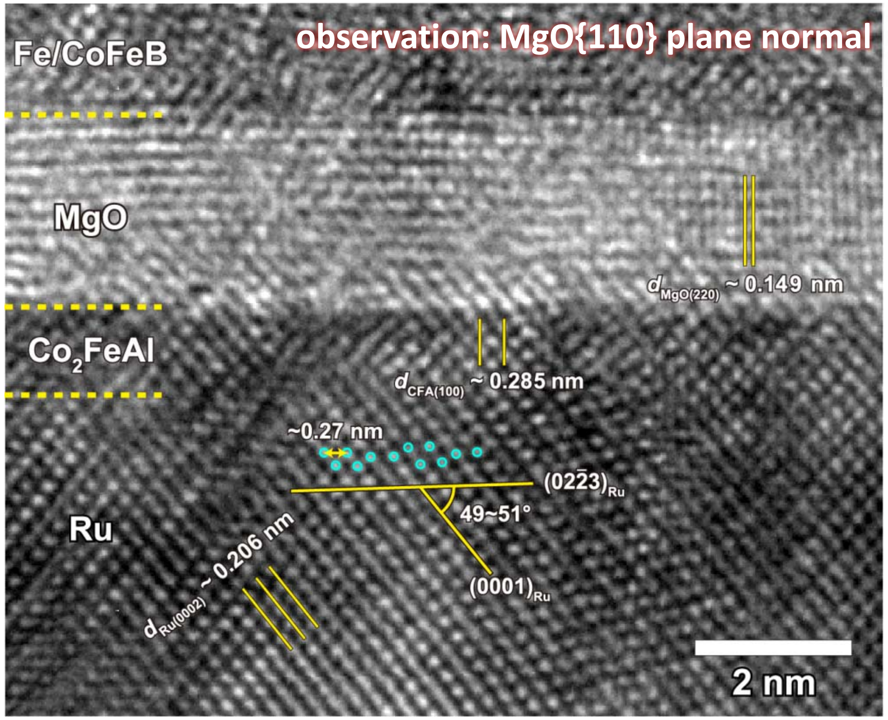

Model (Bulk hcp-Ru)

a_{Ru} = 0.2704 nm
c_{Ru} = 0.4278 nm

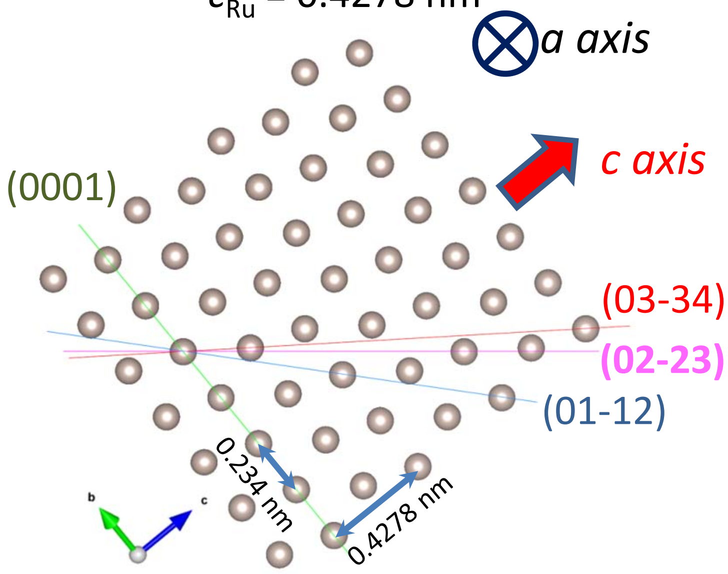

∠(0001)-(02-23): **50.61°**
∠(02-23)-(03-34): 3.26°
∠(02-23)-(01-12): 8.20°

Nano electron-beam diffraction

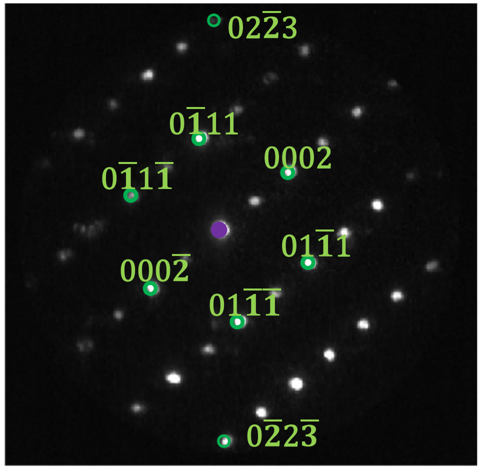

Nearly Ru$(02\bar{2}3)$ growth

(To be more accurate, $(03\bar{3}5)$ growth)

Why do CFA and MgO grow epitaxially on it?

Epitaxial relationship of MgO/Ru/CFA heterostructure

Plan view for Ru(02$\bar{2}$3)

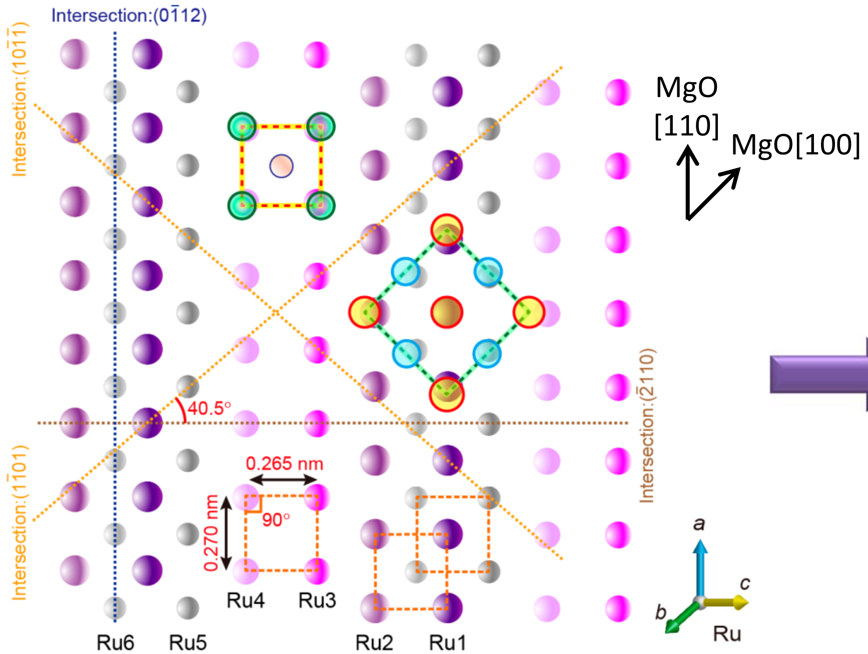

Side view

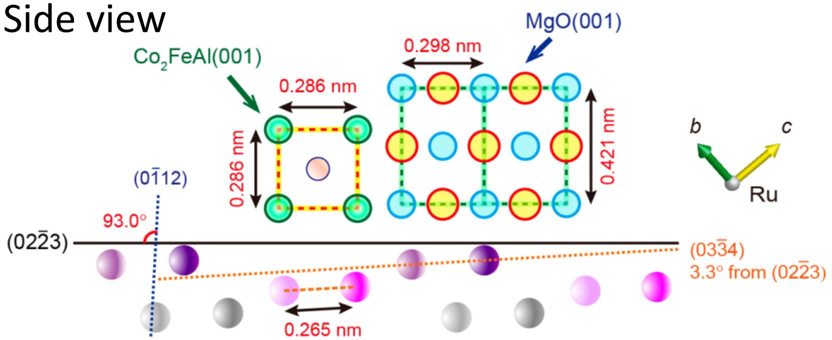

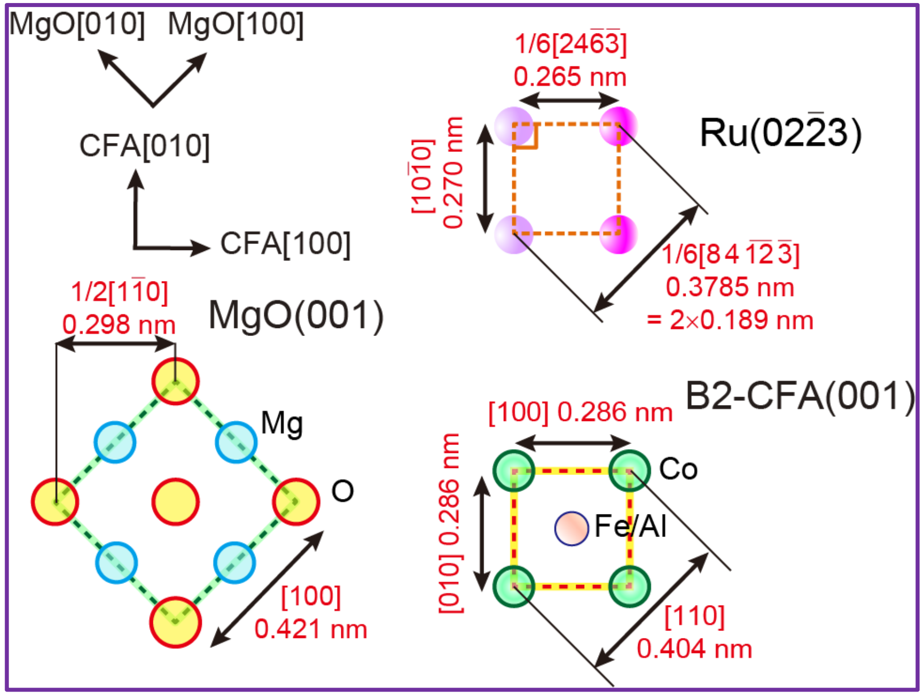

- Epitaxial relationship: MgO(001)/Ru(02$\bar{2}$3)/CFA(001)
- Lattice mismatch
  - **~11% (MgO/Ru)**
  - **~8% (Ru/CFA)**

cf. ~5% (MgO/Cr), ~1% (Cr/CFA)

Nearly square lattice structure of the Ru plane can act as a template of the CFA(001) growth

Negligible effect of buffer/CFA interface to i-PMA

Cr/CFA/Cr

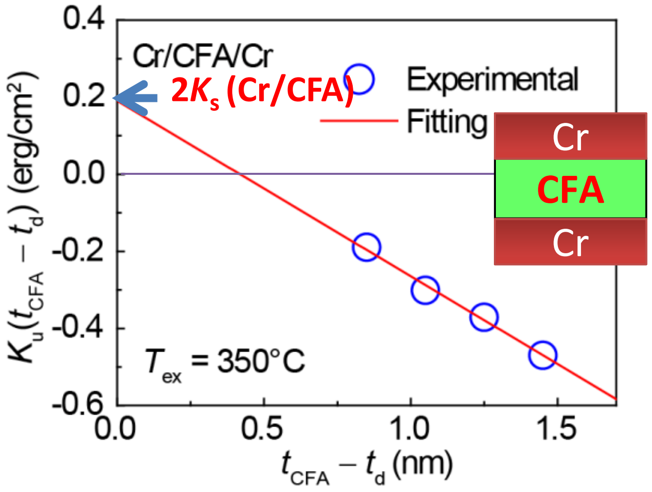

Ru/CFA/Ru

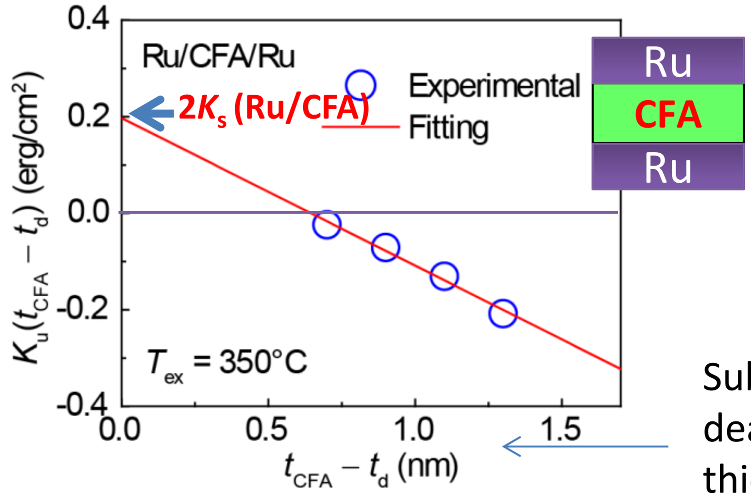

Subtraction of dead layer thickness: t_d

Both Cr/CFA and Ru/CFA interfaces show negligible contribution to interface-PMA

K_s (Cr or Ru/CFA) ~ 0.1 erg/cm^2

cf. CFA/MgO interface: K_s = 1.0 erg/cm^2 (Cr-buffer), 2.2 erg/cm^2 (Ru buffer)

Possible origin of the enhanced PMA:
Improvement of CFA/MgO lattice combination due to a weaker effect from the Ru lattice

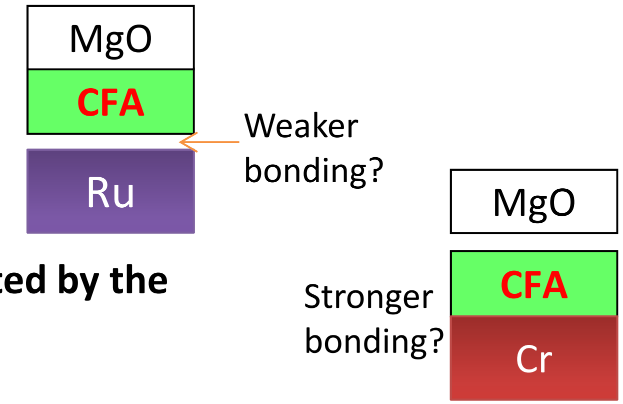

cf. Cr buffer: CFA lattice with a structure of **Cr/CFA/MgO is dominated by the Cr(001) lattice** owing to the very small lattice mismatch
= not a perfect CFA/MgO interface (related to lattice distortion)

Large TMR ratio in a Co_2FeAl/MgO/CoFeB p-MTJ

Z. C. Wen *et al.*, Adv. Mater. **26**, 6483 (2014).

Ru/CFA (1.2)/MgO (1.8)/Fe (0.1)/$Co_{20}Fe_{60}B_{20}$(1.3 nm) p-MTJ

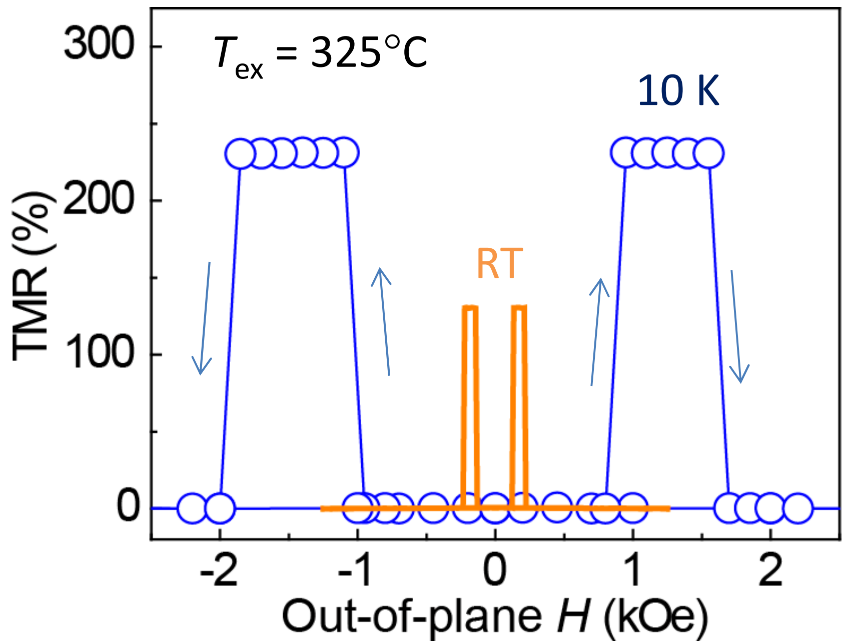

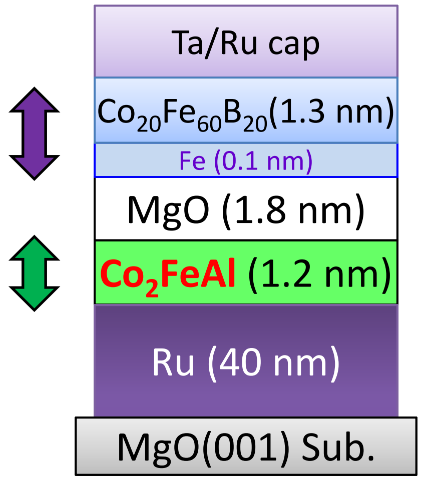

TMR: 132% at RT (237% at 10 K)

(Cr-buffer: 91% at RT)

Over 130% TMR at RT
in p-MTJ using the interface PMA of Co_2FeAl/MgO

The epitaxial Ru with a high crystal index opens up a new path in the development of engineered heterostructures combining hcp and cubic or tetragonal materials.

Outline

Possible origin of i-PMA in bcc-Fe/MgO system

K. Nakamura *et al.*, PRB **81**, 220409(R) (2010).

Hybridization between oxygen and Fe atoms shifts up m = 0 ($3d_{z2}$) above E_F

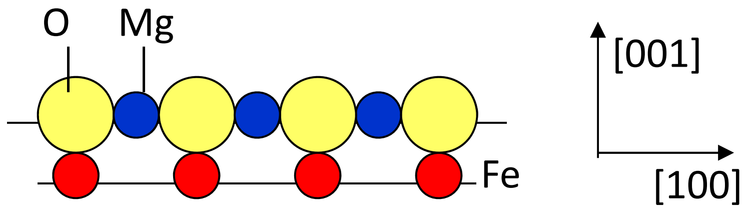

(a) Fe/MgO

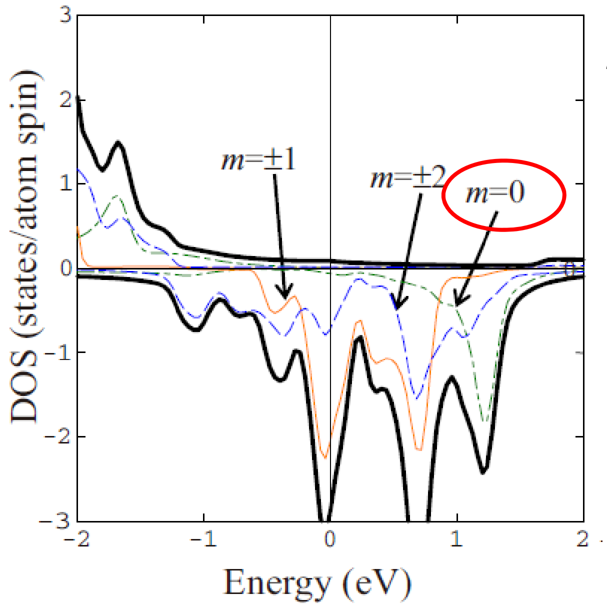

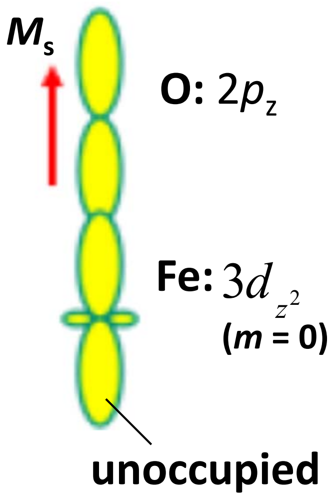

Hybridization between **oxygen $2p_z$** and **Fe $3d_{z2}$** orbitals plays an important role for PMA in the Fe/MgO system

H. X. Yang *et al.*, PRB **84**, 054401 (2011).

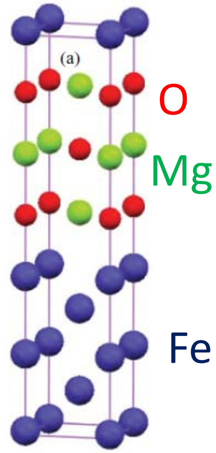

TABLE I. PMA value (erg/cm^2) and magnetic moment m [μ_B per Fe(Co) atom] for different layers of Fe(Co) in Fe(Co)|MgO magnetic tunnel junctions under different oxidation conditions.

	Fe|MgO			Co|MgO:
	Pure	Underoxidized	Overoxidized	pure
PMA	2.93	2.27	0.98	0.38
m (μ_B)				
Interfacial	2.73	2.14	3.33	1.67
Sublayer	2.54	2.41	2.70	1.84
Bulk	2.56	2.55	2.61	1.60

Fe　Co

The calculated PMA energy density of Fe/MgO is much larger than that of Co/MgO

Co_2FeAl = Co rich (50 at.%) alloy

However, the band structures of Co-based Heusler alloys are considerably different from those of Fe or Co owing to their half-metallic properties.

Bruno model:
spin-orbit interaction is treated as a perturbation for the tight binding approximation

Anisotropy of orbital magnetic moments between perpendicular ($m_{orb}^{\perp}$) and in-plane directions ($m_{orb}^{\parallel}$) is proportional to PMA (for 3*d* transition metals).

Angular-dependent x-ray magnetic circular dichroism (XMCD) study

To deduce the **orbital magnetic moments** along perpendicular and in-plane directions

$$K = \alpha\xi(m_{orb}{}^{\perp} - m_{orb}{}^{\parallel})$$

Element specific PMA energy (K)

Spin-orbit splitting (ξ) (33 meV for Fe)

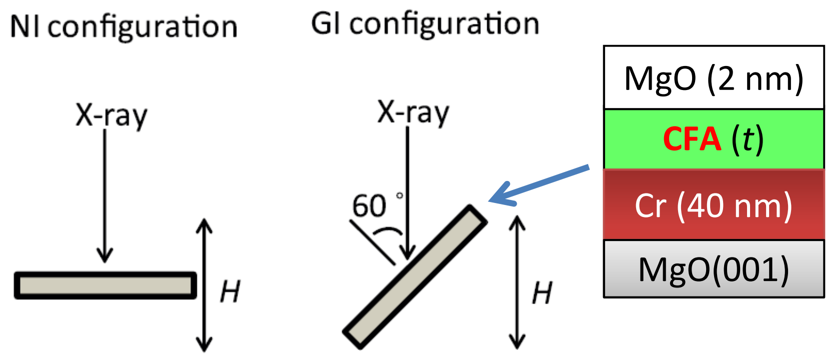

$$m_{orb}(\theta) = m_{orb}{}^{\parallel}\sin^2\theta + m_{orb}{}^{\perp}\cos^2\theta$$

Angular-dependent XMCD study: hybridization Fe-O

In collaboration with Prof. Okabayashi (Univ. Tokyo)
BL-7A in Photon Factory, KEK

J. Okabayashi, HS *et al*., APL**103**, 102402 (2013).

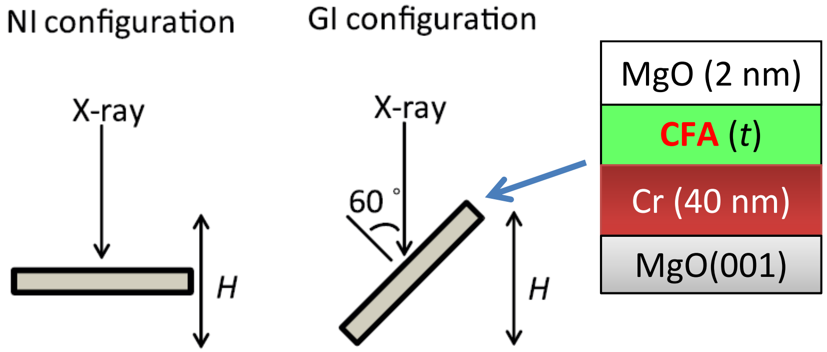

Spectra taken in normal incidence (NI) and grazing incidence (GI) revealed the anisotropic orbital moments.

MgO(001)sub./Cr(40 nm)/CFA(*t*)/MgO(2nm)

$$m_{orb}(\theta) = m_{orb}^{\parallel}\sin^2\theta + m_{orb}^{\perp}\cos^2\theta$$

TABLE I. Spin magnetic moments (m_{spin}) and orbital magnetic moments of parallel and perpendicular components $m_{orb}^{\perp}$, $m_{orb}^{\parallel}$, respectively, of Fe and Co in Co_2FeAl layers of different thickness. The unit is μ_B.

	0.8 nm **PMA**		2 nm ← **in-plane anisotropy**		→ 10 nm	
	Fe	Co	Fe	Co	Fe	Co
m_{spin}	1.83	1.21	2.08	1.22	1.91	1.21
$m_{orb}^{\perp}$	0.32	0.16	0.22	0.14	0.21	0.13
$m_{orb}^{\parallel}$	0.24	0.16	0.21	0.15	0.22	0.13

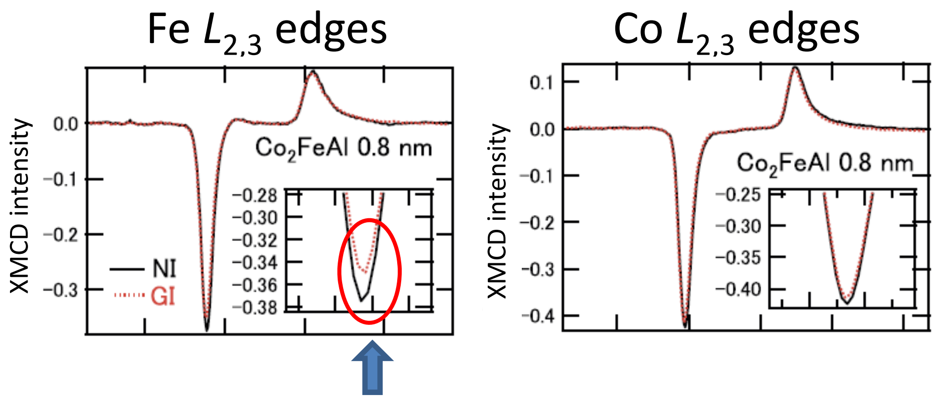

anisotropic orbital moments

Large anisotropic Fe orbital moments at the CFA/MgO interface ($m_{orb}^{\perp}$(Fe) > $m_{orb}^{\parallel}$(Fe))

Bruno model: 0.37 erg/cm² (mJ/m²)

XMCD result suggests contribution of Fe atoms (negligible small for Co) in CFA

Theoretical predictions of PMA at CFA/MgO interface

Ab initio calculation by Prof. Shirai Group (Tohoku U)

D. Mori *et al.*, EB-07, Intermag 2012

PMA arises from **Co-terminated interface** for CFA/MgO(001) system (MgO/$L2_1$-CFA/MgO)

K_s: Interfacial PMA enargy density

Co-terminated case

K_s^{Co} = 0.99 erg/cm² (mJ/m²) --- PMA

FeAl-terminated case

K_s^{FeAl} = –0.49 erg/cm² --- In-plane MA

K_s(exp. Cr-buffered) = 1.0 erg/cm²
K_s(exp. Ru-buffered) = 2.2 erg/cm²

Relevant report

R. Vadapoo, A. Hallal, M. Chshiev (SPINTEC group) arXiv:1404.5646v1

Co-terminated case

K_s^{Co} ~ 1.3 erg/cm² (mJ/m²) --- PMA

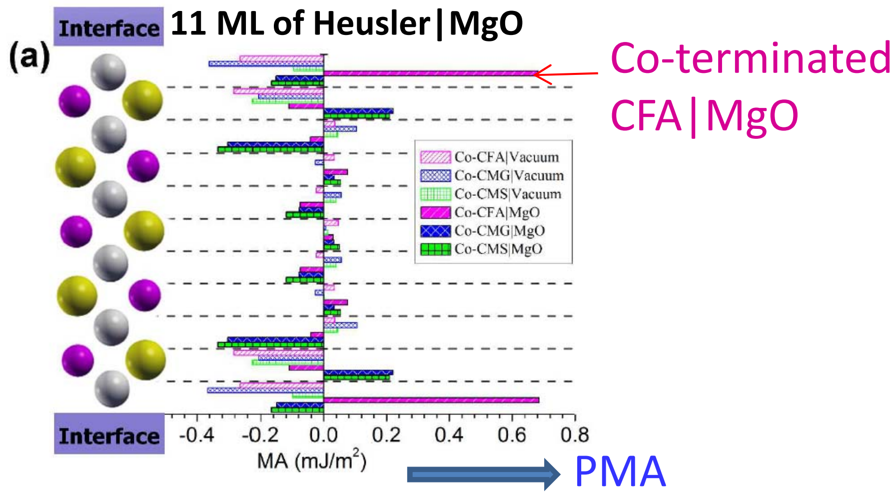

PMA is theoretically expected only in **Co-terminated CFA**, however **FeAl-terminated CFA** is more thermodynamically stable

Atomic model of *B*2-Co_2FeAl(001)

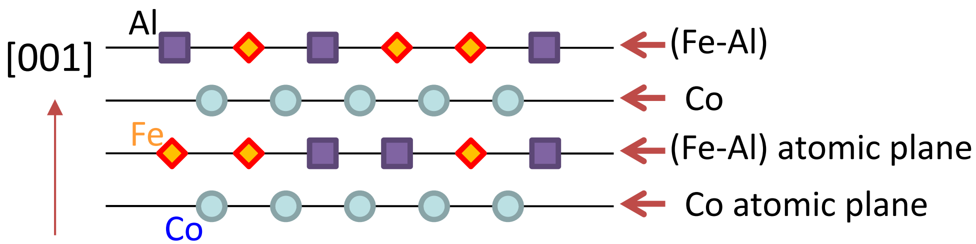

Termination layer of CFA?

Determination of the interfacial structure is needed

Al interdiffusion from CFA layer to MgO barrier

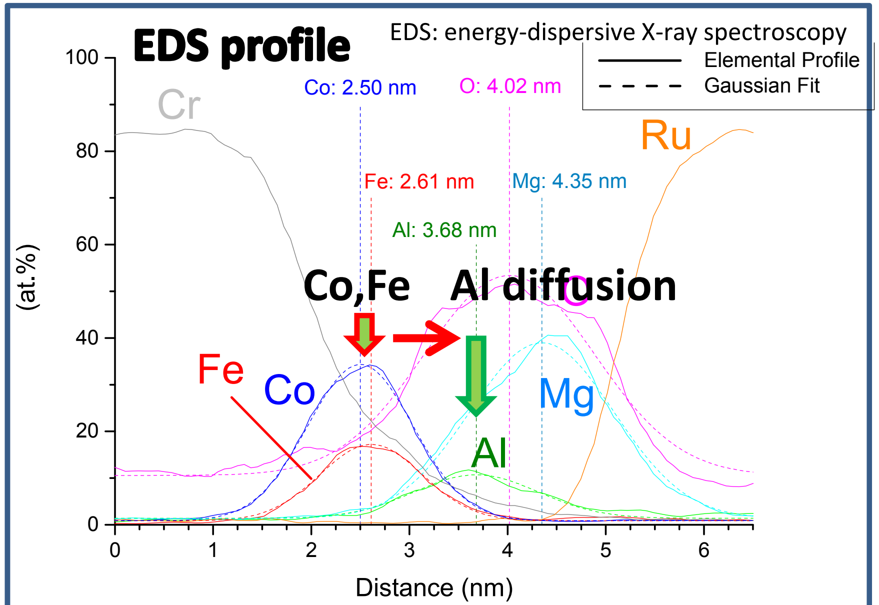

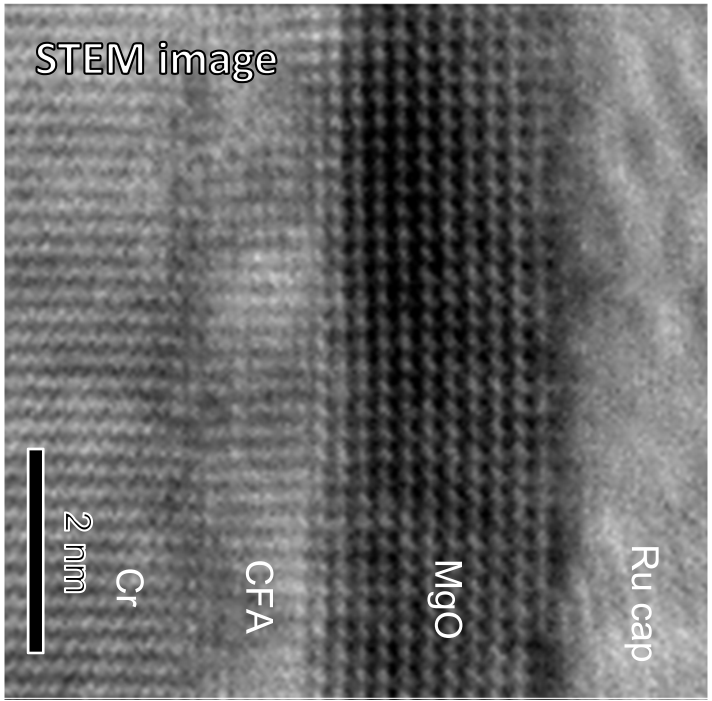

TEM sample

T_{ex}= 350°C

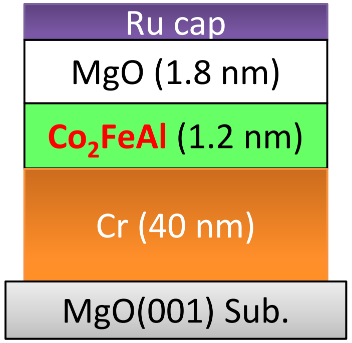

Wen *et al.*, unpublished.

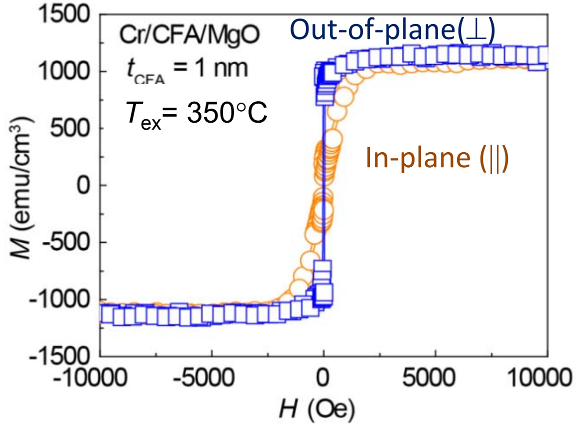

- Significant Al diffusion from CFA into MgO
- The CFA layer is no longer a "Heusler alloy"

Solid-phase reaction at the CFA/MgO interface

Co_2FeAl ➡ **Co-Fe (+Cr, Al)**

MgO barrier ➡ **Mg-Al-O**

Enhancement of hybridization between Fe and O orbitals? (under investigation)

Importance of sub-nm scale structural analyses

Outline

1. Background
   Co_2FeAl Heusler alloy based magnetic tunnel junctions (MTJs) for MRAM applications

2. Perpendicular anisotropy in Co_2FeAl ultra-thin films
   2.1 Perpendicular magnetic anisotropy (PMA) and TMR in ultrathin Co_2FeAl/MgO structures
   2.2 Enhanced PMA by Ru($02\bar{2}3$) underlayer

3. Co_2FeAl MTJs with a lattice-matched $MgAl_2O_4$ coherent barrier (In-plane magnetized MTJ)

T. Scheike

New coherent barrier material: Spinel $MgAl_2O_4$

- *Giant RT tunnel magnetoresistance (TMR)*
- *Non-deliquescence*
- *Tunable lattice parameter: Good lattice matching with 3d ferromagnetic electrodes*

R. Shan, HS *et al*., Phys. Rev. Lett. **102**, 246601 (2009)
H. Sukegawa et al. Appl. Phys. Lett **96**, 212505 (2010), Phys. Rev. B **86**, 184401 (2012)

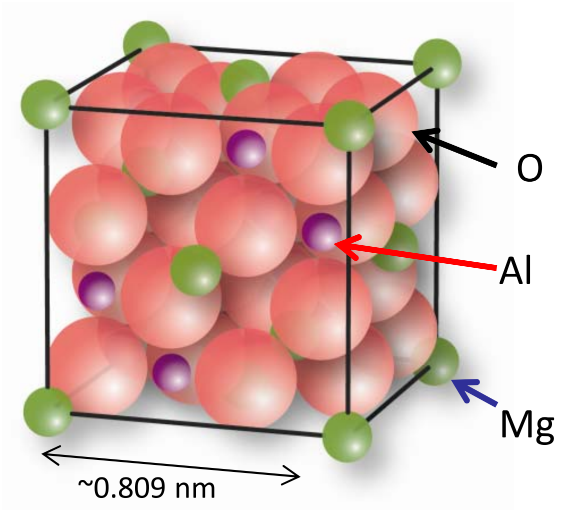

http://commons.wikimedia.org/wiki/File:Spinel2.jpg

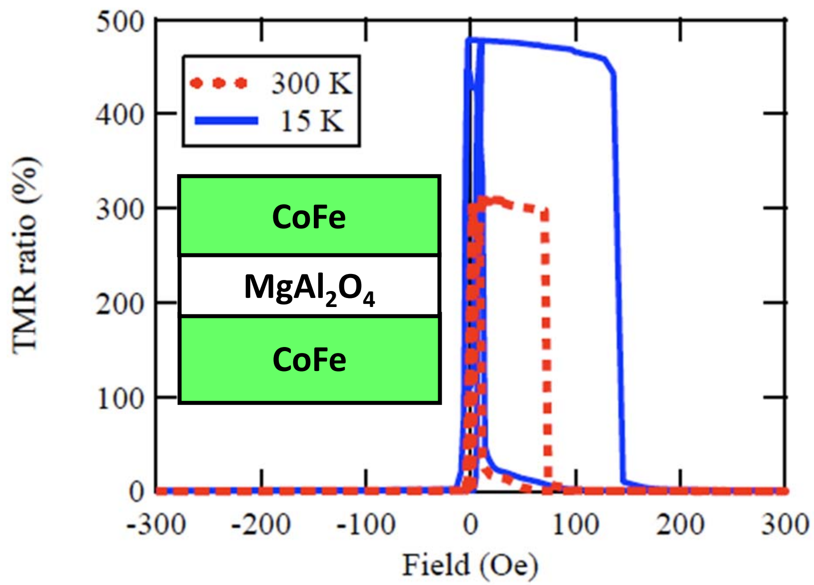

{220} spots: Spinel structure

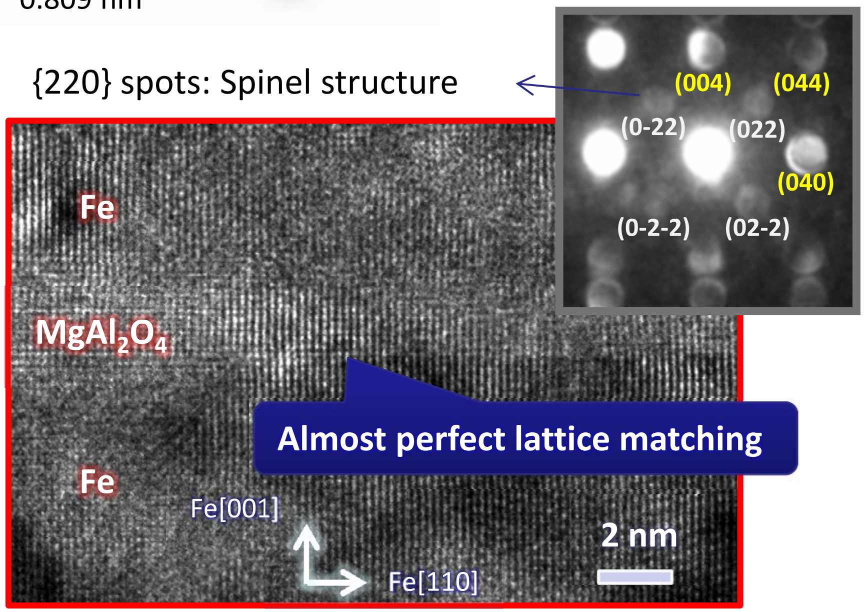

Max TMR ratio : 328 % (RT)
: 494 % (4 K)

Giant TMR owing to coherent tunneling effect in non-MgO barrier

Δ_1 transport mechanism is still valid!

Current status of spinel-based MTJs

Mg-Al film → Post-oxidation → **Crystalline Mg-Al-O(001)**

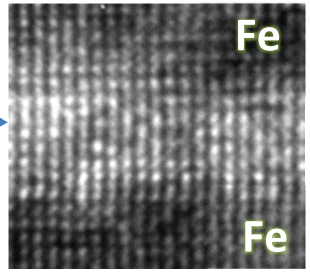

- Perfect lattice matching with 3*d* FM/Co-based Heuser alloys Phys. Rev. Lett. **102**, 246601 (2009).
- Large TMR: >300% Phys. Rev. B **86**, 184401 (2012).
- Wide RA range: 10^0-10^6 $\Omega\cdot\mu m^2$ (STT switching) Appl. Phys. Lett. **103**, 142409 (2013); ibid.**105**, 092403 (2014).
- Interface-induced PMA Status Solidi RRL **8**, 841 (2014).

Lattice mismatch

Electrode materials	Mismatch (%) for (001) growth	
	vs. MgO (0.421 nm)	vs. $MgAl_2O_4$-based (0.396 ～ 0.404 nm)
bcc-Fe (a =0.2866 nm)	–3.8	+0.3 ～ +2.5
$L2_1$-Co_2FeSi (a = 0.564 nm)	–5.3	–1.4 ～ +0.8
$L1_0$-FePt (a = 0.385 nm)	–8.6	–4.8 ～ –2.7
DO_{22}-MnGa (a = 0.390 nm)	–7.4	–3.4 ～ –1.4

Next generation spintronics materials

TMR at RT (CoFe(B) electrodes)

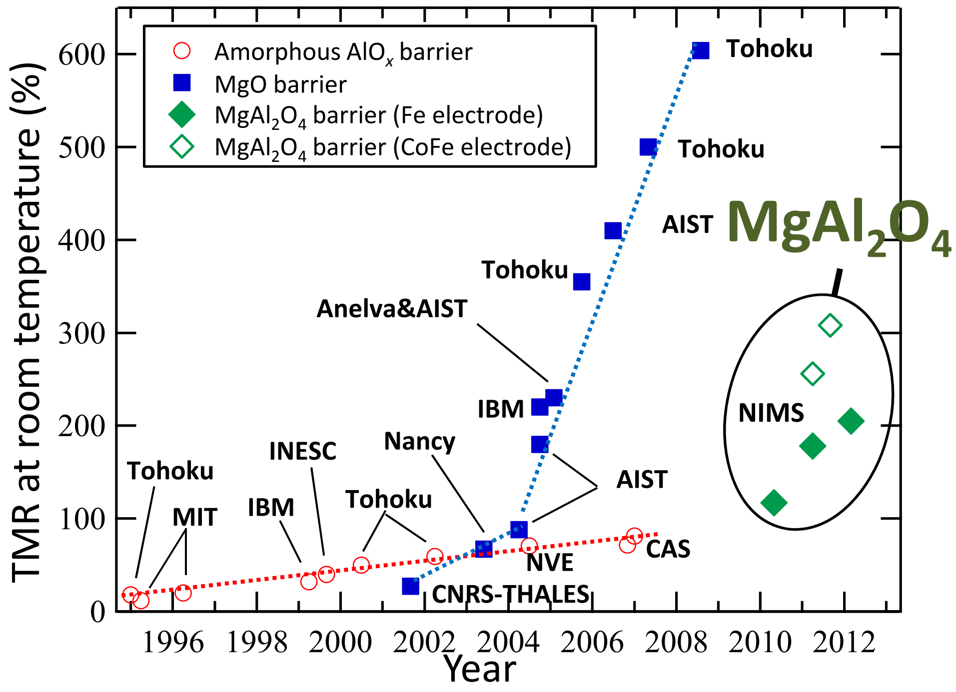

Lattice-matched Heusler $Co_2FeAl/MgAl_2O_4$ MTJs

T. Scheike *et al*., APL**105**, 242407 (2014).

In-plane magnetized MTJ

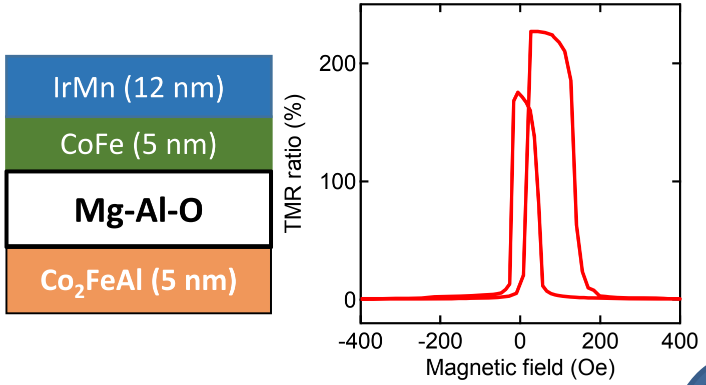

TMR: 236%
RA: 1.8 kΩ·µm²

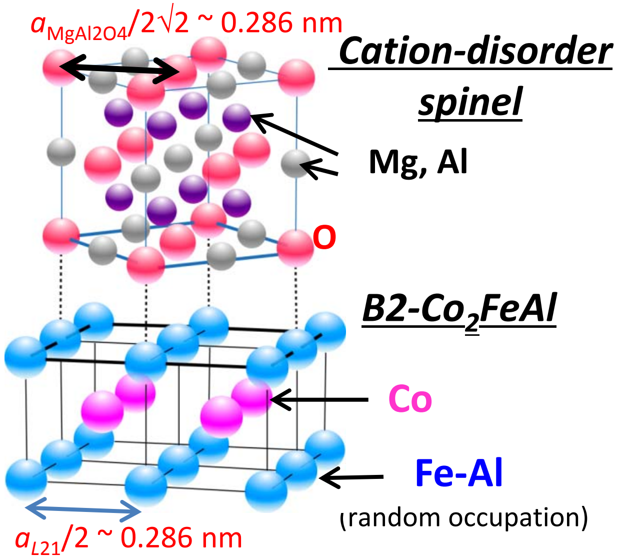

Misfit: ~0% (cf. MgO/CFA ~3.8%)

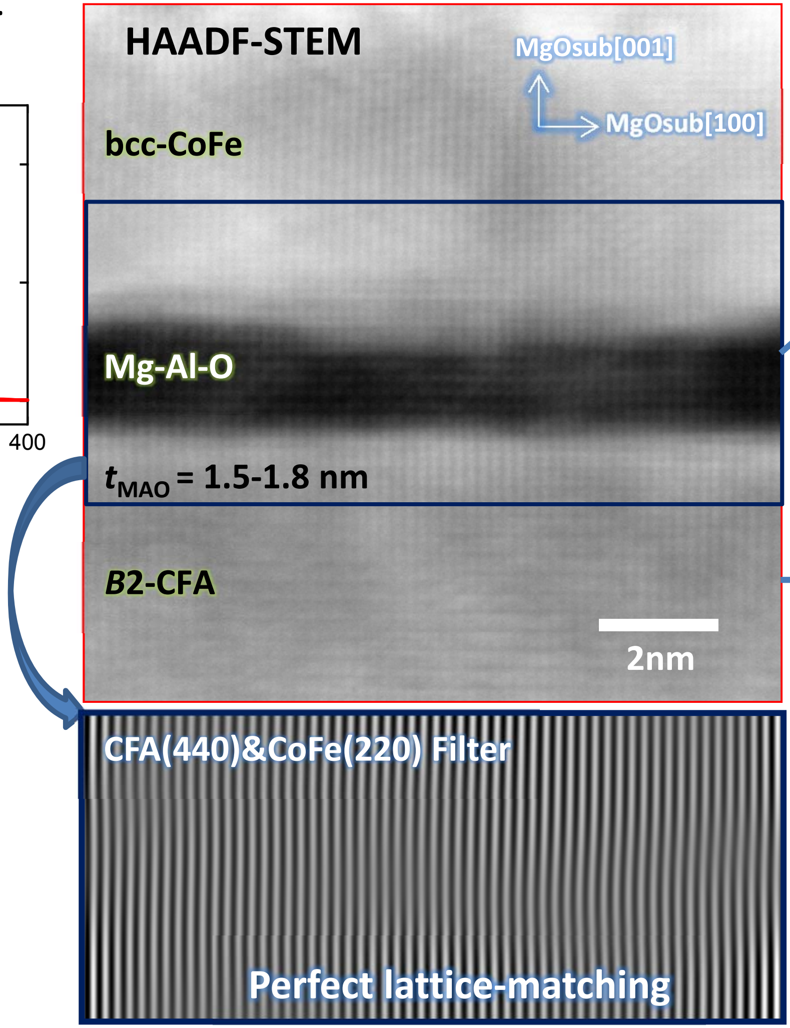

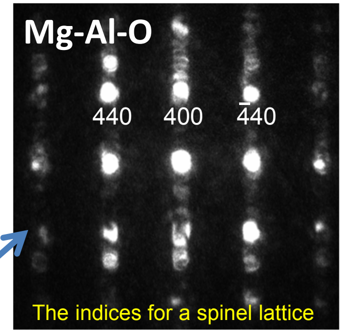

Cation-disorder spinel structure

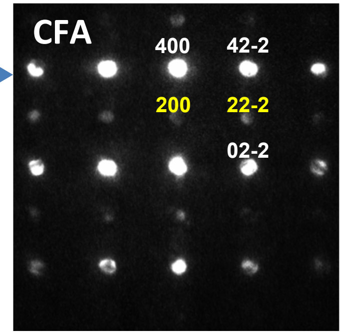

***B2* CFA**

Giant TMR effect in CFA/Mg-Al-O/CoFe MTJs

236-280% TMR at room temperature

Latest data > 340%

Conclusion

Co_2FeAl-based heterostructures

Interface-induced PMA

(1) Perpendicular magnetic anisotropy in a Cr/Co_2FeAl/MgO (**K_s ~ 1 erg/cm^2**) and p-TMR of **91%** at RT.

(2) Ru buffer layer as a new ferromagnetic layer growth: Unusual crystallographic orientation Ru(02-23) buffer enhanced PMA (K_s ~ 2.2 erg/cm^2) and p-TMR (**132%** at RT)

(3) Al interdiffuction from CFA layer to barrier was confirmed; the Fe-O hybridization owing to the interfacial reaction could be responsible for the strong PMA.

	Cr buffer	Ru buffer
Buffer orientation	bcc (001)	hcp ~(02$\bar{2}$3)
K_u (Merg/cm^3) for 1-nm	0.8	3.1
K_s (erg/cm^2)	1.0	2.2
TMR (%)	91 (RT)	132 (RT)

Review of PMA in CFA-based heterostructures→ Sukegawa *et al.*, SPIN **4**, 1440023 (2014).

Lattice-matched MTJ using Spinel barrier

Lattice-matched CFA/$MgAl_2O_4$/CoFe MTJs were successfully developed and giant TMR more than 280% at RT was demonstrated.

CFA-based (or CFA-derived) heterostructures will be a promising candidate for future spintronics applications

New perpendicular magnetization material: *N-deficient MnGaN*

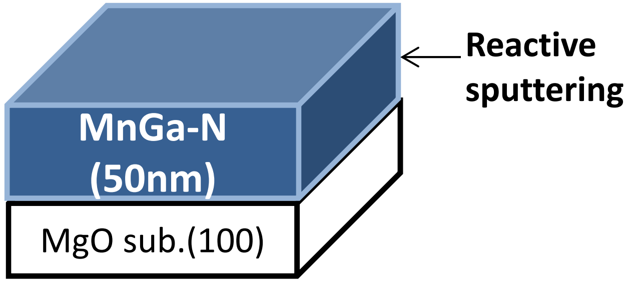

D0_{22}-Mn_3Ga (tetragonal *L*2_1)

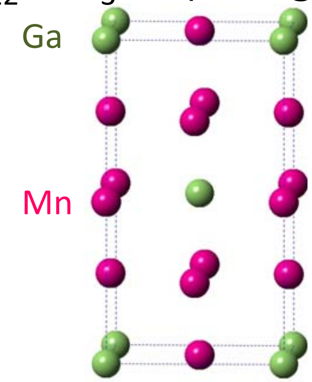

N introduction

Anti-perovskite Mn_3GaN

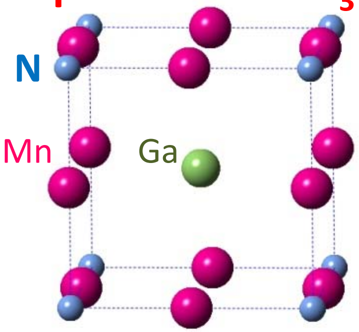

(bulk Mn_3GaN: **antiferromagnet**)

$Mn_{57}Ga_{32}N_{11}$ (**N-deficient**, but structurally homogeneous)

XRD

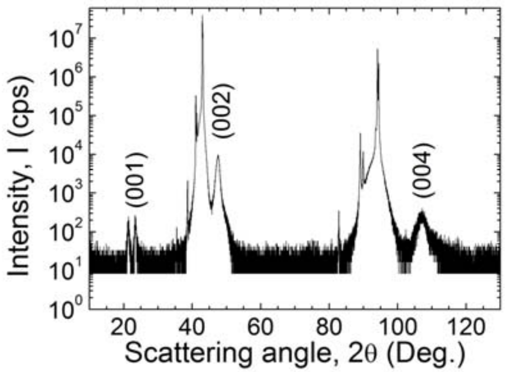

Antiperovskite (*E*2_1) single phase

***M-H* loops**

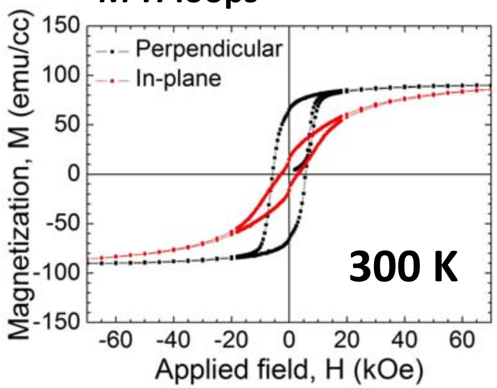

PMA film

Cross-sectional TEM

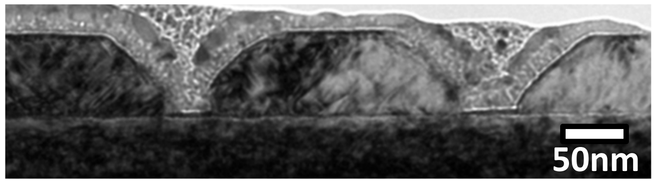

D0_{22}-MnGa: very rough

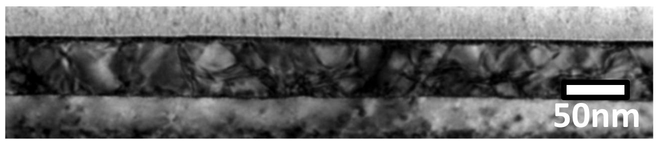

***E*2_1-MnGaN: atomically flat**

- Ferromagnetic MnGaN with PMA (K_u ~ 0.2 MJ/m^3)
- Flat film structure
- Low saturation magnetization (~100 emu/cc)
- Curie temperature >> room temperature
- Relatively high spin-polarization ~ 57% (PCAR)

New PMA material for spintronics

Lee *et al.*, APL**107**, 032403 (2015).